

Aziz Danyal (Orcid ID: 0000-0002-0734-6894)  
Hassan Daniyal (Orcid ID: 0000-0001-8812-7230)  
Johnson Ryan C (Orcid ID: 0000-0003-2195-739X)

## Data-Driven Modeling to Enhance Municipal Water Demand Estimates in Response to Dynamic Climate Conditions

Ryan C. Johnson, Steven J. Burian, Carlos A. Oroza, Carly Hansen, Emily Baur, Danyal Aziz, Daniyal Hassan, Tracie Kirkham, Jessie Stewart, Laura Briefer Alabama Water Institute (Johnson), University of Alabama, Tuscaloosa, Alabama, USA; Civil, Construction and Environmental Engineering (Burian, Aziz), University of Alabama, Tuscaloosa, Alabama, USA; Civil and Environmental Engineering (Oroza, Baur, Hassan), University of Utah, Salt Lake City, Utah, USA; Oak Ridge National Laboratory (Hansen), Oak Ridge, Tennessee, USA; Salt Lake City Department of Public Utilities (Kirkham, Stewart, Briefer), Salt Lake City, Utah, USA (Correspondence to Johnson: rjohnson18@ua.edu).

**Research Impact Statement:** Increasing model complexity with climate variables and data-driven models advances seasonal municipal water system demand estimate accuracy to enhance management decision-making in a changing climate.

### ABSTRACT

Altered precipitation and temperature patterns from a changing climate will affect supply, demand, and overall municipal water system operations throughout the arid western U.S. While supply forecasts leverage hydrological models to connect climate influences with surface water availability, demand forecasts typically estimate water use independent of climate and other externalities. Stemming from an increased focus on seasonal water demand management, we use the Salt Lake City, Utah municipal water system as a testbed to assess model accuracy vs. complexity trade-offs between simple climate-independent econometric-based models and complex climate-sensitive data-driven models to average to extreme wet and dry climate conditions – representative of a new climate normal. The climate-independent model displayed low performance during extreme dry conditions with predictions exceeding 90% and 40% of the observed monthly and seasonal volumetric demands, respectively, which we attribute to insufficient model complexity. The climate-sensitive models displayed greater accuracy in all conditions, with an ordinary least squares model demonstrating a measurable reduction in prediction bias (3.4% vs. -27.3%) and RMSE (74.0 lpcd vs. 294 lpcd) compared to the climate-independent model. The climate-sensitive workflow increased model accuracy and characterized climate-demand interactions, demonstrating a novel tool to enhance water system management.

This is the author manuscript accepted for publication and has undergone full peer review but has not been through the copyediting, typesetting, pagination and proofreading process, which may lead to differences between this version and the Version of Record. Please cite this article as doi: [10.1111/1752-1688.13186](https://doi.org/10.1111/1752-1688.13186)

*Keywords:* Machine Learning, Climate Resilience, Water Demand Projections

## INTRODUCTION

The nexus surrounding supply and demand in the arid western U.S. continues to be a considerable water resources challenge, displayed by extensive infrastructure to store and deliver water (Gleick, 2010; Dawadi & Ahmad, 2012). For example, there are nearly 11,000 water storage reservoirs in the western U.S., with the three largest river systems (i.e., Columbia, Colorado, and Missouri) combined storage capacity approaching 185,000 Mm<sup>3</sup> (USBR, 2023). The extensive infrastructure addresses the differential timing of snowmelt-driven streamflow in the spring with heavy summer water use, and supports multiyear storage for prolonged drought (Christensen et al., 2004; Rajagopalan et al., 2009; Stern & Sheikh, 2021). For municipal water systems (MWS), the persistent summer drought and high evapotranspiration drive increases in outdoor water use from April to October to maintain landscaping health (UDNR, 2014; Opalinski et al., 2020). With climate change altering the surface water yields of critical western U.S. catchments and cost and feasibility constraints hampering new source and infrastructure development (Brown et al., 2019), there is a shift to explore demand management for operational, tactical, and strategic MWS management decisions (Gleick, 2010; Ryu et al., 2012; Olmstead, 2014).

Demand management leverages water demand estimates (e.g., monthly, annual, total volume) to support MWS decision-scaling, capacity planning, conservation efforts, and overall operations (Donkor et al., 2014). Statistical time-series models can estimate short- (< 1 day) to long-term (> 10 years) water use projections based on historical use trends with high accuracy (Ghiassi et al., 2008; Arandia et al. (2015)), assuming serial correlations between demand and seasonality will only deviate through efficiencies in water use (Billings & Jones, 2011). While these econometric-based methods can produce high accuracy, the arid western U.S. exhibits high

water use seasonality, and because of a changing climate, irrigation season length and intensity deviate from historical use patterns (Finch et al., 2016; Snyder et al., 2019; Opalinski et al., 2020). Regional seasonality, global climate anomalies (e.g., ENSO), and a changing climate challenge the use of serial correlation models, autoregressive models, and/or models neglecting climate influences (Matthews et al., 2011; Koutsoyiannis & Montanari, 2014).

Integrating features describing MWS service area characteristics and change within the model workflow can improve prediction accuracy, connecting climate influences and urbanization pathways to changes in water demand (Coomes et al., 2010; Opalinski et al., 2020). Polebitski and Palmer (2010) integrated city size and sector composition, population characteristics, rainfall and temperature, the marginal price of water, and socioeconomic factors describing the municipal service area into their demand model to increase forecasting accuracy. Identifying and integrating key influencers of municipal demand is becoming increasingly important in arid and semi-arid regions, where limited supplies and high per-capita water use determine water system performance (Hirsch, 2011; Zhao et al., 2018) and where there is a need to develop contingency plans to mitigate supply-demand deficits during hydrological drought (Blanc et al., 2014).

Building on the relationships between MWS service area dynamics and water demand, machine learning (ML) algorithms have advanced short- and long-term water demand forecasting accuracy (Adamowski & Karapatki, 2010; Behboudian et al., 2014; Ghalehkhondabi et al., 2017; Vijai & Sivakumar, 2018; Antunes et al., 2018; Altunkaynak & Assefa, 2018). W. Li and Huicheng (2010) demonstrated a 6% reduction in annual demand uncertainty for Dalian City, China by using fuzzy neural networks (vs. using linear regression methods) with socioeconomic, climate, and other related demand-influencing features. Tiwari and Adamowski (2014) developed an artificial neural network (ANN) to forecast weekly to monthly demands to advance operational forecasting

accuracy (< 3% error). Although ML can deliver accurate water system demand estimates, ML algorithms are susceptible to overfitting, can produce unreasonable estimates from inputs exceeding the bounds of training data (e.g., a changing climate leading to temperatures exceeding those observed in the historical record), and the black box from high model complexity obscuring the relationships between input variables, model algorithm, and predictions (Riter & Munoz-Carpena, 2013). The documented limitations of ML have resulted in a reluctant adoption within MWSs for examining system performance and informing decision-making (Donkor et al., 2014).

The complex interactions between arid western U.S. climate, service area characteristics, and modeling methodology highlight a research gap surrounding the prediction accuracy of seasonal municipal demand, specifically, to current and projected conditions influenced by a changing climate while considering model complexity vs. accuracy trade-offs. Integrating model complexity as an evaluation measure allows for a methodological investigation of accuracy changes to different model formulations, with an operational preference for algorithms with high accuracy and low complexity. Lower complexity models generally offer greater interpretability, a less intensive development time, and are more computationally efficient (Makridakis et al., 2018; Shrestha & Mahmood, 2019). We define model complexity as the number of parameters within the model and translate the complexity to the interpretability given by the number of parameters, consistent with the ML community (Guidotti et al., 2018; Barceló et al., 2020). Addressing the research gap, we pose two research questions surrounding model complexity and variations in seasonal climate conditions concerning arid western U.S. municipal water use:

- Is there a measurable change in seasonal water demand forecasting accuracy from more complex climate-sensitive models compared to climate-independent econometric-based models for arid western municipal water systems under extreme climate conditions?

- Are there measurable changes in prediction skill from models of differing levels of complexity for estimating demands to various climate regimes?

We investigate the research questions using Salt Lake City Department of Public Utilities (SLCDPU) as a case application, where we develop climate-independent econometric-based models, to be referred to as climate-independent models, and data-driven climate-sensitive modeling workflows. The objective is to characterize climate-independent model accuracy for estimating municipal demands and use a data-driven climate-sensitive modeling workflow to advance the prediction accuracy to different climate conditions. We train a lower complexity Ordinary Least Squares (OLS) model and develop complex Random Forest Regression (RFR) and multilayered perceptron (MLP) models to address the research questions. The research motivation is to advance the understanding of climate influences on the water system and develop tools to support sustainable water system management.

## METHODS

### *Study Area*

We use SLCDPU as a representative arid western U.S. water system because of its seasonality, high summer water use, interannual climate variability, and urbanized landscape (serving 350,000 people), recognizing that demands, their specific influences, and the resulting accuracy in modeling demands will vary between water systems. The long-term records of water use support the development of the climate-independent and climate-sensitive models, and to investigate model forecasting accuracy to seasonality, year-to-year climate changes, and climatic extremes synonymous with climate change. Due to the proximity of SLCDPU to the Wasatch Mountains, there is a strong dependence on winter snowpack for supply that strongly influences seasonal and year-to-year surface water supply availability (Smith et al., 2015; Brooks et al., 2021).

The mountain snowpack functions as a natural storage reservoir, with the streamflow from City (CC), Parleys (PC), Big Cottonwood (BCC), and Little Cottonwood (LCC) creeks providing approximately 60% of the annual supply (Figure 1) (Khatri et al., 2018). Valley groundwater withdrawal and interbasin water transfers, both driven by snow-dominated hydrology, complete the remaining 40% of the annual water supply (Figure S1) (Collins & Associates, 2019).

Four distinct seasons influence SLCDPU water demands: a snowy winter with no irrigation; a hot, dry summer with high evapotranspiration and irrigation use; and wet spring and fall periods that define the beginning and the end of the irrigation season (UDNR, 2010). Temperatures exceeding 35.0°C throughout the summer result in up to 1000 mm of irrigation applied between April to October, contributing to Utah routinely ranking as a top five highest per-capita water use state in the country (Dieter, 2018). Idaho, Wyoming, Arizona, Nevada, Colorado, Oregon, and Montana exhibit similar water use, with these western states ranked as the top ten highest per-capita water use states in the nation (Maupin, 2018).

SLCDPU has reported the total volume of monthly treated water releases into the distribution system to the Utah Division of Water Rights from 1980 to the present (UDWR, 2023), consisting of residential, institutional, and commercial uses and including leakage and unaccounted-for system losses. Figure S2 decomposes water use by sector, indicating residential outdoor water use as the dominant sector (e.g., 44%). Municipal demand has decreased from 1100 lpcd to 800 lpcd over the past two decades, reducing per-capita demand by 25% (Figure S3). Table 1 displays the statistical summary of SLCDPU water use from April to October, highlighting the high seasonal and annual variability because of outdoor demands. Per-capita water use is a function of the total water delivered into the water system divided by the service area population (i.e., Salt Lake City, Holladay, Cottonwood Heights, and Millcreek)..

[Insert Figure 1, JAWRA\_RJohnson\_Fig1.pdf here]

[Insert Table 1 here]

### *Climate-Independent Demand Modeling*

Climate-independent water demand model development aligns with the methods described in Billings and Jones (2011) and we calculate the monthly liters per-capita day water (lpcd) use from the training period spanning from 1980-2017, omitting the testing scenarios and disregarding years with missing observations. The model relies upon serial correlation, estimating monthly demands as a function of the historically observed monthly climate-demand interactions and the assumption that previous observations will reflect future demands based on Equation 1

$$\overline{lpcd}_m = \frac{\sum_{i=1}^n lpcd_m}{n} \quad (1)$$

where  $m$  refers to the month of interest and  $n$  refers to the number of years in the training period, which consists of 30 years of training data ( $n$ ). While small fluctuations in indoor water use from November to March occur, we assume consistent per-capita water use during this period (i.e., 590 lpcd). Table 2 displays the historical monthly per-capita demands for SLCDPU.

[Insert Table 2 here]

### *Climate-Sensitive Demand Modeling*

The motivation of the climate-sensitive modeling workflow is to connect dynamic climate conditions to monthly outdoor per-capita water use from April to October. We create service area climate and urbanization features as model inputs and apply dimensionality reduction techniques to optimize the model features. The climate-sensitive models use the same features and training data, consistent with the 30 years of data used to develop the climate-independent models.

**Data and Feature Engineering.** Data preparation for modeling outdoor demands requires separating indoor water use from total water use, with the assumption that indoor plus outdoor water use equals total municipal water use. We assume indoor water use activities (e.g., showers, dishwashing, laundry) remain relatively constant throughout the year (Jacobs and Haarhoff, 2007; Lee et al., 2011) and that there is minimal water applied for outdoor purposes from November to March. With these assumptions, we calculate monthly per-capita indoor use with Equation 2

$$\overline{D_{I_y}} = \frac{D_{Nov_{y-1}} + D_{Dec_{y-1}} + D_{Jan_y} + D_{Feb_y} + D_{Mar_y}}{5} \quad (2)$$

where  $\overline{D_{I_y}}$  is the mean annual indoor per-capita water use for the respective year ( $y$ ). We calculate monthly outdoor water use ( $D_{O_m}$ ) using Equation 3

$$D_{O_m} = D_{T_m} - \overline{D_{I_y}} \quad (3)$$

where  $\overline{D_{I_y}}$  is the indoor water use from Equation 2,  $D_{T_m}$  is the total per-capita demand, and  $m$  is the month of interest. The outdoor demand (lpcd) of each month forms the dependent variable for training climate-sensitive models.

Feature engineering seeks to develop independent variables that improve water demand modeling skill. We create temperature, precipitation, snowfall, and streamflow features to represent the dynamic climate conditions and conservation guidelines, land-cover type, population, and housing features as these features can be strong predictors of municipal water demand (Polebitski & Palmer, 2010; Tiwari & Adamowski, 2014; Oyebode & Ighravwe, 2019).

Precipitation and temperature are critical features reflecting seasonal climate influences on demand and we use the North American Land Data Assimilation System (NLDAS) climate-forcing data products to retrieve temperature and precipitation estimates (Xia et al., 2012). We calculate monthly air temperature (°C) and precipitation (mm) features as a function of the spatial

average of the service area from March through October – one month before and extending through the end of the irrigation season. While there are many in-situ weather stations, the NLDAS data products broaden the transferability of the framework to other water systems.

Mountain streamflow represents the complex interactions among mountainous topography (e.g., snowdrift, aspect, and microclimates), variable winter precipitation patterns (e.g., global climate oscillations), snowmelt (e.g., timing, duration, and quantity), and the mountain hydrology (e.g., groundwater and baseflow) that contribute to supply availability (Scalzitti et al., 2016; Bohne et al., 2020; Brooks et al., 2021). We calculate monthly streamflow ( $\overline{Q_{cms}}$ ) from the daily discharge measurements at the canyon mouths of the four supply streams using the United States Geological Survey (USGS) and Salt Lake County monitoring stations before extensive water diversion. While nearly a complete time series, we interpolate the few missing daily values as a function of up or downstream measurements per the methods from Hughes and Smakhtin (1996).

We create snowfall features as an indicator of the climate anomaly (e.g., wet, average, or dry winters). Although temporally separate from summer outdoor use and different than the precipitation metrics, snowfall can indicate high-elevation watershed supply availability (Shukla et al., 2011; Peters-Lidard et al., 2021) and we used November to April monthly and seasonal snowfall from the Alta Guard station (NOAA, 2023) to form the snowfall features. While there are four key watersheds for SCLDPU, year-to-year variability is highly correlated between watersheds due to the proximity of their headwaters and we use the features to differentiate year-to-year climate conditions rather than characterize the physical volume of water per watershed.

We incorporate antecedent climate features to reflect the hydrological system memory, specifically, that previous precipitation and temperature conditions affect future soil moisture conditions and irrigation needs (Potts et al., 2006; J. Li et al., 2020). The antecedent climate

features begin in March, before the irrigation season, and incrementally increase in number per month until October. For example, the antecedent climate features of October include March, April, May, June, July, August, and September precipitation, temperature, and streamflow features in addition to October precipitation, temperature, and streamflow features.

Complementing the climate features, we develop density-based population and housing features to reflect urbanization and as a generalizable metric to compare with other municipalities. We use the population and housing estimates from the U.S. Census (Census, 2023) to calculate population and housing densities based on the boundaries of the SLCDPU service area (204 km<sup>2</sup>). Since census data is not continuous, we use linear interpolation between decadal census observations to create a continuous population (p) and housing (H) dataset.

Agricultural, residential, and urban land uses can influence municipal water use (Donnelly & Cooley, 2015). At a five-year frequency, beginning in 1985 and including 2017, we retrieve USGS Landsat 5 and 8 surface reflection tier 1 satellite imagery to determine land cover/land use changes within the service area boundary. We select images between September and November to assist algorithm training and delineate between irrigated vs. non-irrigated and vegetated vs. non-vegetated land covers. The September to November imagery emphasizes irrigated areas within the 520-560 nm wavelengths, contrasting against dead grass and non-irrigated vegetation. We adjust the blue, green, and red bands with the parameters of 500 (min), 3000 (max), and 1.4 (gamma) for Landsat 5. All parameters remain the same for Landsat 8 images, except for the max parameter increasing to 5000 to match the pixel attributes of Landsat 5 images. We process all images as recommended by USGS for shadow and cloud removal (USGS, 2019a, 2019b) and use the Sci-Kit learn Random Forest classifier version v0.21.3 to create features as the percentage of the urban

area, residential area, irrigated area, and vegetated area, further described in the *Supplementary Information* (Buitinck et al., 2013; Rodriguez- Galiano et al., 2012; Zhu et al., 2012).

The Utah Department of Water Resources established a statewide goal to reduce per-capita water use by 25% by 2025 (UDWR, 2019), and we develop a conservation feature ( $C_m$ ) to represent the anticipated monthly reductions in demand based on the goals. The conservation features uses the long-term average demand of each month from the 1980-2000 period as the baseline and determine the monthly 25% reduction goal for 2025. We use linear interpolation between 2001 to 2025 to create a continuous time series of conservation goals using Equation 4

$$C_m = \overline{D_m} - \frac{\overline{D_m} * 25\%}{25 \text{ yrs}} * y \quad (4)$$

where  $C_m$  is the conservation feature,  $m$  refers to the month of interest,  $\overline{D_m}$  is the mean per-capita water use of month  $m$  for the 1980-2000 period, and  $y$  is the number of years past the year 2000. The conservation feature aligns with western U.S. water conservation policies and the adoption of linear conservation goals to achieve substantial long-term reductions (UDWR, 2019; CWCB, 2015; SNWA, 2019). Municipalities not using a constant rate may explore a constant percent rate reduction, which would form the feature (U.S. EPA, 1998). Figure S3 displays the conservation trend for SLCDPU, along with year-to-year variability in annual water use.

**Feature Selection.** Feature selection reduces model dimensionality, improves learning accuracy, and facilitates a better model understanding (Cai et al., 2018). We use Recursive Feature Elimination (RFE) due to the algorithm prioritizing dimensionality reduction through the identification of strong predictors to improve model skill, even in the presence of highly correlated features (X.-w. Chen & Jeong, 2007; Lin et al., 2012; Hamada et al., 2021). The RFE algorithm removes noisy and non-informational variables, selecting stronger features than other methods such as Lasso penalized logistic regression or Random Forest (Tolosi & Lengauer, 2011).

Implementing a correlation bias reduction (CBR) strategy into the feature selection workflow can further improve model performance and we adapt the CBR algorithm introduced by Yan and Zhang (2015), as displayed in Equations 5 – 11

$$CBR(F_{m_{in}}, D_m, T_{m_{tc}}, T_{m_{fc}}) = F_{m_{out}} \quad (5)$$

Where  $m$  is the month of interest,  $F_{m_{in}}$  are all the potential features,  $D_m$  is the target demand,  $T_{m_{tc}}$  is the threshold for determining the minimum correlation between features and demand,  $T_{m_{fc}}$  is the threshold for determining the maximum correlation between two features, and  $F_{m_{out}}$  are the highly correlated features to the target demand ( $D_m$ ) with minimal correlation to another. The first step is to select features with a correlation greater than  $T_{m_{tc}}$  to the respective monthly demand

$$f_{m_{out}} = i \in F_{m_{in}} \mid |\rho(i, D_m)| > T_{m_{tc}} \quad (6)$$

where  $f_{m_{out}}$  are the features with a correlation greater than  $T_{m_{tc}}$  with demand. The Pearson correlation coefficient determines the correlation between features to target and feature to features

$$\rho = \frac{\sum_i (f_i - \bar{f})(y_i - \bar{y})}{\sqrt{\sum_i (f_i - \bar{f})^2} \sqrt{\sum_i (y_i - \bar{y})^2}} \quad (7)$$

where  $\rho$  is the Pearson correlation coefficient to measure the linear association between features ( $f_i$ ) to target ( $y_i$ ) or feature ( $f_i$ ) to features ( $y_i$ ). Using  $f_{m_{out}}$ , the algorithm selects for features that correlate less than  $T_{m_{fc}}$

$$f_{m_{out2}} = j \in f_{m_{out}} \mid |\rho(j, f_{m_{out}})| < T_{m_{fc}} \quad (8)$$

where  $f_{m_{out2}}$  are the features from  $f_{m_{out}}$  that exhibit a correlation with another less than  $T_{m_{fc}}$  (e.g., not highly correlated). If two features exhibit a correlation greater than  $T_{m_{fc}}$ , the algorithm selects the features with a greater correlation with the demand ( $D_m$ ) of month  $m$  from  $f_{m_{out}}$

$$f_{m_{out3}} = k \in f_{m_{out}} \mid |\rho(k, f_{m_{out}})| > T_{m_{fc}} \quad (9)$$

where  $f_{m_{out3}}$  are the features ( $f_{m_{out}}$ ) with a greater correlation to another than  $T_{m_{fc}}$ . The function then selects features with a greater correlation with the demand ( $D_m$ ) of month  $m$  from  $f_{m_{out3}}$  using

$$f_{m_{out4}} = l \in f_{m_{out3}} \left| |\rho(l, D_m)| > n \in f_{m_{out3}} \right| |\text{corr}(n, D_m)| \quad (10)$$

where  $f_{m_{out4}}$  are the features with the greater correlation with the demand ( $D_m$ ) from  $f_{m_{out3}}$ . For example, if features  $l$  and  $n$  exhibit a correlation to another greater than  $T_{m_{fc}}$  and feature  $l$  exhibits a greater correlation with  $D_m$  than  $n$ , then  $l$  joins the  $f_{m_{out4}}$  group and the *CBR* function removes  $n$  as a potential feature. With the features in  $f_{m_{out2}}$  and  $f_{m_{out4}}$  with greater than the minimum correlation threshold ( $T_{m_{tc}}$ ) to demand ( $D_m$ ) and a feature-to-feature correlation of less than  $T_{m_{fc}}$ , the algorithm determines the *CBR* features by

$$F_{m_{out}} = f_{m_{out4}} + f_{m_{out2}} \quad (11)$$

The *CBR* process selects demand-correlated features  $F_{m_{out}}$  with acceptable levels of collinearity (i.e.,  $<10$ ) to pass to RFE (Song & Kroll, 2011).

We use Scikit-learn 0.24.1 RFE to identify the optimal monthly per-capita outdoor demand predictors (Pedregosa et al., 2011). The algorithm uses a grid search function to assign feature importance weights and recursively prune the number of features over five-fold cross-validation to optimize the feature set. We perform an exhaustive grid search using RFE over a range of target correlation thresholds ( $T_{m_{tc}}$ , 0-0.7 in 0.05 increments) and feature correlation thresholds ( $T_{m_{fc}}$ , 0.65-0.90 in 0.05 increments), with the CBR-RFE framework identifying the optimal predictors of monthly demand to train the climate-sensitive OLS, MLP, and RFR models.

**Ordinary Least Squared Regression.** We use the Scikit-learn OLS algorithm for its interpretable statistical relationships between predictors and demand (i.e., variable coefficients),

providing a formal representation of the observed interactions to mitigate the black box of ML algorithms. The generalized monthly OLS regression formula is

$$lpcd_m = \beta_1 x_1 + \beta_2 x_2 + \dots + \beta_n x_n \quad (12)$$

where  $m$  is the month of interest,  $\beta_n$  are the coefficient weights, and  $x_n$  is the predictor of interest. We train the OLS model using five-fold cross-validation and fit without a y-intercept to characterize the influence of each predictor on demand. For example, if July air temperature is a key predictor of July demand, the coefficient will communicate the statistical relationship between a projected 1°C increase in July temperature on July per-capita day (lpcd) demand with respect to the other features. We apply the Statsmodels v0.12.2 package to communicate a 95% prediction confidence level based on the internally characterized model error (Seabold & Perktold, 2010) and the number of features in the final model determines model complexity.

**Random Forest Regression.** We use the tree-based RFR algorithm to represent one of two complex machine learning models for its proficiency in water resources modeling applications (Tyralis et al., 2019). RFR uses a meta-estimator of several fitted decision trees on multiple subsamples of the training data and then averages to improve prediction accuracy and overall robustness (Biau & Scornet, 2016). We use the Scikit-Learn RandomForestRegressor package (Pedregosa et al., 2011) to train the model using a five-fold cross-validation and a GridSearchCV function to optimize the hyperparameters: number of estimators 5-75 at 5-unit intervals, max depth 2-40 at 2-unit intervals, and max predictors 0.2 - 0.8 at 0.2-unit intervals. The function evaluates model performance via a “fit” and “score” method for all possible hyperparameter combinations, with the final hyperparameters demonstrating the least internal model error. The number of trees in the optimized model (i.e., the number of estimators) determines model complexity.

**Multilayered Perceptron.** An MLP model serves as the second complex ML algorithm and demonstrates high performance across many water resources applications (Hastie et al., 2009; Sit et al., 2020). We use the Keras package within TensorFlow v2.4.1 (Abadi et al., 2015) to build the MLP network, consisting of an input layer that receives the optimized predictors, middle hidden layers with nodes/neurons that form the computational engine, and an output layer that produces the prediction. Model training consisted of the following parameters: relu activation function, eight hidden layers with neurons ranging from 8 to 128, the Adam optimizer, and 500 epochs. Model training used five-fold cross-validation with backpropagation gradient descent to weigh the network and minimize error and the total number of model weights from the layer-node combinations determines the model complexity.

#### *Evaluation Scenarios and Metrics*

Given the proximity to and the dependence of SLCDPU to the surface water supplies from the adjacent mountains, we use seasonal accumulated snowfall ( $S_{cm}$ ) as the metric to characterize the climate and establish wet, dry, and average testing. Seasonal accumulated snowfall describes the climate, as it bridges the gap between climate conditions and surface water supply (Rosenberg et al., 2011; Fleming et al., 2021). We use the observations from Alta Guard station (40.5905°N, -111.638°E, 2,656 m) located within the headwaters of LCC to identify the most recent wettest (2008), driest (2015), and average (2017) seasonal snowfall. We performed a Log Pearson type III analysis using the 78 years of observations to determine the dry scenario (680 cm) and wet scenario (1,660 cm) have a 150-year and 15-year return period, respectively, a significant departure from the historical mean (1,262 cm) and consistent with a changing climate (Khatri et al., 2018; Naz et al., 2018; Brown et al., 2019). We include an average climate state (1,347 cm) as a reference point to compare performance with extreme scenarios. Complementing the dry, average, and wet climate

conditions, we use the climate conditions from 2018-2022 to extend the model evaluation period and assess the skill of each method to year-to-year variations in climate, filling in the gap between extremely wet and extremely dry (Table 3). The 30 years of observations and 8 years of testing resulted in an 80%/20% training/testing split that is consistent with ML model development (Pham et al. 2020; Moayedi et al. 2020). The temperature, precipitation, and surface water supply observations from each scenario drive the climate-sensitive models and we determine model performance using the observed monthly per-capita demands attributed to each scenario.

**[Insert Table 3 Here]**

We use percent bias (PBias), root-mean-squared-error (RMSE), and Kling-Gupta Efficiency metrics (KGE) metrics to determine model performance to the three climate states (i.e., wet, average, dry), the average performance across the three climate states, and the average performance over the 2018-2022 period. Evaluating model performance across the different climate conditions highlights the predictive performance one can expect for each modeling method to the year-to-year variability in arid western U.S. climate. Motivated to enhance seasonal MWS guidance, we do not model finer resolution (e.g., daily) demands because we are not concerned with daily water use fluctuations or the effects of individual precipitation events. Complementing the model performance metrics, we include the volumetric percent error of seasonal and annual demand estimates to further exemplify the operational strengths and limitations of each method.

**Percent Bias (PBias).** PBias computes the average amount that the observed is greater or lesser than predicted as a percentage of the absolute value of the observed. PBias communicates if, on average, the model favors predictions above (- bias) or below (+ bias) the observed, with ideal *PBias* values close to zero.

$$PBias = \frac{100\%}{n} \sum_{i=1}^n \frac{(y_i - f_i)}{|y_i|} \quad (13)$$

where  $f_i$  are the predicted values and  $y_i$  are the observed for timestep n.

**Root Mean Squared Error (RMSE).** RMSE aggregates the magnitude of residuals for all data points into a single quantitative measure of performance, with values closer to zero indicating a greater model accuracy (Fisher, 1920).

$$RMSE = \sqrt{MSE} = \sqrt{\frac{\sum_{i=1}^n (f_i - y_i)^2}{n}} \quad (14)$$

**Kling-Gupta Efficiency Metric (KGE).** KGE is an expression of the distance between the point of ideal model performance in the space described by: 1) correlation, 2) variability, and 3) bias (Gupta et al., 2009). KGE values approaching 1 indicate a perfect model fit; a benchmark of -0.41 indicates an overall performance greater than the mean (Knoben et al., 2019).

$$\beta' = \frac{\mu_f}{\mu_y} \quad (15)$$

where  $\beta'$  is the bias ratio,  $\mu$  is the mean target value ( $f$  for predicted and  $y$  for observed).

$$\alpha = \frac{\sigma_f}{\sigma_y} \quad (16)$$

where  $\alpha$  is the variability ratio and  $\sigma$  is the standard deviation of the predicted and observed values.

$$\rho = \frac{\sum_i (f_i - \bar{f})(y_i - \bar{y})}{\sqrt{\sum_i (f_i - \bar{f})^2} \sqrt{\sum_i (y_i - \bar{y})^2}} \quad (17)$$

where  $\rho$  is the Pearson correlation coefficient to measure the overall strength of a linear association between predicted ( $f_i$ ) and observed ( $y_i$ ), and KGE being the lowest score of its components

$$KGE = 1 - \sqrt{(\rho - 1)^2 + (\beta' - 1)^2 + (\alpha - 1)^2} \quad (18)$$

## RESULTS/DISCUSSION

### *Climate-Independent Demand Estimates*

The climate-independent model produces demand estimates greater than the observed for all scenarios (Figures 2 & 3), with the PBias metric characterizing the prediction trend at -27.3%

and -19.0% for the three climate conditions and the 2018 - 2022 period (Table 4), respectively. The highest prediction accuracy was during the wet scenario, displayed by an approximate 50% reduction in PBias and RMSE, along with an increase in KGE (i.e., 0.81 vs. 0.67). We observed the average and dry climate conditions challenging model accuracy with errors approaching 90% or 700 lpcd, and a large PBias of -39.7% and 33.4% for the dry and average conditions, respectively. The dry and average climate conditions resulted in greater than a 100% increase in error compared to the wet scenario and strongly biased overall model performance. A high negative PBias with the demand estimates for 2021 and 2022 (-30% and -40%, respectively) is consistent with the average and dry conditions. The KGE exceeds the acceptable prediction threshold of -0.41 but the overall error indicates a poor model fit.

**[Insert Table 4 Here]**

**[Insert Figure 2, JAWRA\_RJohnson\_Fig2.pdf Here]**

**[Insert Figure 3, JAWRA\_RJohnson\_Fig3.pdf Here]**

The climate-independent model error compounds when scaling predictions to monthly, seasonal, and annual volumetric demands. The overall model error (i.e., RMSE of 294 lpcd) results in an overprediction of seasonal demand by 6.5 Mm<sup>3</sup> (8%), 24.2 Mm<sup>3</sup> (34%), and 20.8 Mm<sup>3</sup> (31%) for the wet, dry, and average conditions, respectively (Table 5). The model similarly overestimates volumetric water demand during the 2018-2022 period by an average of 22% or 17.4 Mm<sup>3</sup>/yr. The annual volumetric error during the dry conditions (i.e., 32.8 Mm<sup>3</sup>) exceeds the storage capacity of the Dell reservoir system (i.e., 27.1 Mm<sup>3</sup>), challenging the utility of the demand estimates for decision support and extending to include financial operations. For example, the revenue projections will exceed the realized monetary resources by \$33,000 - \$66,000 (e.g., 32.9 Mm<sup>3</sup> ×

0.01 - 0.02 \$/m<sup>3</sup> (Salt Lake City Department of Public Utilities, 2022)) during the dry scenario and the municipality may have purchased unnecessary supplies to mitigate anticipated deficits.

**[Insert Table 5 Here]**

*Climate-Sensitive Demand Estimates*

The climate-sensitive models translated the climate influences on water demand with high prediction accuracy (Figures 2 & 3). The predictions were close to the observed, displayed by PBias values of 3.4%, -2.5%, and 1.7% for the OLS, MLP, and RFR models, respectively, over the wet, dry, and average climate conditions (Table 4). The RFR model produced a lower PBias and greater KGE than the OLS and MLP models during the wet conditions while the OLS model produced a lower PBias and greater KGE than the RFR and MLP during the average and dry conditions. The dry scenario presented challenging conditions for the MLP and RFR models, displayed by a PBias of -13.8% and -7.5%, and KGE decreases to 0.68 and 0.82, respectively. The OLS model displayed the highest model accuracy during the dry climate conditions, with a low PBias (0.20%), RMSE (48.4 lpcd), and high KGE (0.98).

The 2018-2022 period examines the impacts of inputs outside of the training bounds on model skill and we observed a decrease in prediction accuracy. The MLP model displayed the least performance of the climate-sensitive models with an increasingly negative PBias (-6.0% vs. -2.5%), an increase in RMSE (237 lpcd vs. 153 lpcd), and a reduction in KGE (0.62 vs. 0.86) compared to the wet, dry, and average scenarios. The MLP model overpredicted June through September demands during the average and dry climate conditions of 2021 and 2022 by up to 50%. The OLS and RFR models displayed similar performance for the 2018-2022 period with a PBias less than 1%, RMSE around 170 lpcd, and a KGE close to 0.80. The OLS and RFR models overpredicted June through September demands for 2021 and 2022 but to a lesser degree than the

MLP model. The consistent over-prediction is likely due to Salt Lake County conserving water amid a multiyear drought, noted by a 13% reduction in water use (Salt Lake County, 2021).

Addressing research question 1, the seasonal and annual error reductions from the climate-sensitive models, specifically the OLS and RFR models, during climate extremes demonstrate a measurable improvement in the model skill compared to the climate-independent model. The reduction in error exceeds the Dell reservoir system storage capacity (i.e., 27.1 Mm<sup>3</sup>) during the dry scenario, exemplifying the strengths of the climate-sensitive modeling framework. The MLP model demonstrated greater accuracy than the climate-independent model but exhibited a reduction in model accuracy during the 2018-2022 period compared to the OLS and RFR algorithms. Based on the model evaluation, the strength in connecting climate conditions to demand estimates becomes more substantial as conditions trend drier.

#### *Model Accuracy vs. Complexity*

There is a substantial variation in the model complexity between each method. The climate-independent model has a complexity degree of 1 (i.e., monthly demand), the OLS algorithm has a complexity degree of 18 (i.e., the number of non-zero model coefficients), the MLP model has a complexity degree of 33,721 (i.e., number of parameters), and the RFR model has complexity degree of 60 (i.e., number of trees). Model accuracy was consistent across all scenarios, with the greatest to least accuracy as follows: OLS, RFR, MLP, and climate-independent models. There were minimal differences in accuracy between the OLS and RFR climate-sensitive models.

A qualitative evaluation of model complexity can bridge the research to operations boundary by understanding how the number of parameters relates to model interpretability and model accuracy (Barceló et al., 2020). The climate-independent model is the least complex due

to the demand estimate being historical monthly mean demand (Equation 1). While simple, the method ignores which can measurably improve prediction accuracy.

The OLS model is the second least complex model with its eighteen predictors but provides the greatest interpretability because of the statistically-derived coefficient relationships between predictors and demand, Table 6. We observe twelve of the eighteen predictors connecting service area monthly air temperature and precipitation to demand, expressing the importance of climate features in the SLCDPU demand modeling framework and exemplifying the benefits of the interpretable predictor-target relationships. For example, for every degree increase in April mean temperature (°C), SLCDPU can expect a 21.3 lpcd increase in April demand. The positive feedback between temperature and demand aligns with the observed patterns of outdoor water use, where high temperatures and minimal precipitation require substantial irrigation (>1000 mm) to maintain landscape health. The statistical relationships between predictors and demand can further support the adoption of climate-sensitive modeling methods in water system management, especially when the model coefficients align with water system operator experience.

The RFR and MLP are the most complex models and due to the number of model parameters (e.g., model weights), the models offer minimal interpretability. The RFR does provide feature importance scoring that indicates the relative importance of a predictor and model logic from the training data but has been shown to not represent model logic outside of the training bounds (Strobl et al., 2008; Tyralis et al., 2019; Drobnič et al., 2020). The MLP is the least interpretable due to the unknown relationships between climate to demand (i.e., black box), only communicating the model performance from training. Model development intensity and computational efficiency can differentiate model complexity trade-offs (Al-Jarrah et al., 2015; Shrestha et. al., 2019), however, the climate-sensitive models took approximately the same time

to develop because of automated training algorithms and predicted in under 1 second, resulting in negligible differences in development and computational efficiency.

**[Insert Table 6 Here]**

Addressing research question 2, we find that there can be measurable improvements in model accuracy by increasing model complexity. The OLS model demonstrated a measurable improvement in prediction accuracy from increased model complexity compared to the climate-independent model. The OLS model demonstrated that sufficient complexity could match or exceed the performance of greater complexity models (i.e., MLP, RFR), making the model a likely tool to assist in water system management. The RFR and MLP models did not produce measurable gains in model accuracy compared to the OLS model, indicating that the largest gains in model accuracy stem from the integration of key, temporally dynamic service area characteristics.

*Benefits of Increased Model Complexity for Water System Management*

A strength of the more complex models is linking water use behavior to the climate conditions, quantifying the influence of air temperature and precipitation changes on monthly, seasonal, and annual demand estimates. From the OLS model, we identify three key climate-demand relationships that improve the understanding of SLCDPU water demands; 1) monthly precipitation and mean air temperature are the strongest determinants of monthly per-capita demand, 2) spring climate conditions play a pivotal role in overall water use, and 3) antecedent climate conditions demonstrate a strong influence on June through September demands. For example, the model identifies a negative precipitation to demand feedback connecting moist spring conditions with prolonged cloud cover and above-average precipitation (e.g., reduced evapotranspiration) to reductions in seasonal water use and dry, warm, and sunny conditions with

increased water use. The climate-demand relationships provide system management with a conceptual understanding of the interactions between climate, seasonality, and water use.

A benefit of including climate influences when estimating season demands is to support water system decision-making. Should the demand projections exceed the estimated supply availability, concerning streamflow timing and storage, an alternative source or contract may be a mitigation strategy. The results indicate that climate-sensitive demand estimates become more essential and representative during drier, supply-limited conditions, a condition where there is an increased need for additional supplies and/or demand hedging to prevent system deficits.

A climate-sensitive demand modeling workflow can produce long-term climate-influenced demand estimates to examine the impacts of a changing climate on MWS performance. By applying a range of climate scenarios, climate-sensitive models can generate a range of demands reflecting the influences of different climate futures on municipal water demands to support planning activities ranging from seasonal outlooks to long-term climate resilience. For example, Figure 4 demonstrates a range of seasonal demands from the OLS model driven by historically observed air temperature and precipitation anomalies.

**[Insert Figure 4, JAWRA\_RJohnson\_Fig4.pdf Here]**

#### *Opportunities to Improve the Climate-Sensitive Modeling Workflow*

The climate-sensitive models demonstrate improved model accuracy compared to the climate-independent models but there remains an opportunity to advance the overall modeling framework. We can no longer assume indoor demands are independent of dynamic service area conditions, as errors in November through March demands indicate the potential effect of water-saving measures due to public drought awareness (Parker & Wilby, 2013; Moglia et al., 2018). There is the potential for a non-linear conservation trend, as a negative exponential trend partially

describes the observed error as each scenario nears the long-term reduction goal year (i.e., 2025). Future research exploring different conservation metric formulations and integrating service area characteristics for indoor demand modeling may improve overall modeling performance, leading to improvements in overall demand prediction accuracy (equation 3).

While the OLS model demonstrated the greatest overall performance for the SLCDPU system, applying the climate-sensitive workflow to other systems may indicate a non-linear predictor-demand relationship that challenges linear regression-based algorithms. We encourage developers to explore many ML algorithms that increase prediction accuracy under non-linear relationships (G. Chen et al., 2017b; Desai & Ouarda, 2021). Examining several ML architectures supports a comprehensive model accuracy vs. complexity comparison to select the optimal model and/or develop an ensemble demand forecasting to produce a range of demand estimates (Al-Sultani et al., 2021; Granata & Di Nunno, 2021; Mosavi et al., 2021).

Decomposing sector water use and including demographic and socioeconomic components could improve model skill by reflecting changes within the service area, as demonstrated by Vijai & Sivakumar (2018) considering census blocks. If the data is available, partitioning water use by sector could refine demand estimates and we expect smaller spatial scales to identify urban, residential, irrigated, and vegetated areas as strong demand predictors. The SLCDPU service area scale likely did not identify these features as strong predictors due to a greater explanatory relationship between the climate and demand compared to land cover changes. For long-term assessments concerning climate and/or urbanization pathways, a range of demographic and socioeconomic shifts could occur and influence the demands (Behboudian et al., 2014).

Risk-tolerance-based decision-making encourages the use of probabilistic predictions (Towler et al., 2013, Quilty et al., 2019). A probability distribution (e.g., Gaussian) of temperature

and precipitation forcings to drive the climate-sensitive model or using probability-based ML algorithms (e.g., Gaussian Process Regression) could generate a probable range of demands (Y. Wang et al., 2014). As an alternative or complement to ensemble methods, probabilistic estimates could support the climate-sensitive modeling workflow for water system management and informed decision-making regarding future climate and urbanization pathways.

## CONCLUSION

This research investigates model complexity vs. accuracy trade-offs considering the linkages between climate and seasonal water demands for arid western U.S. municipal water systems. The substantial year-to-year climate variability of Salt Lake City Department of Public Utilities serves as a case study to explore the prediction accuracy limitations of climate-independent models (i.e., low complexity) and demonstrate how increases in model complexity (i.e., novel data-driven climate-sensitive model frameworks) can increase prediction skill. Using testing scenarios examining model skill to extreme wet to extreme dry climate conditions, we find the climate-independent model to overestimate monthly demands up to 90% and seasonally up to 40%. We attribute the errors to low model complexity and identify potentially severe management implications concerning supply acquisition, budgeting, and overall water system management as climate conditions trend toward a drier state. We develop climate-sensitive water demand models using ordinary least-squared (OLS), multilayered perceptron (MLP), and random forest (RFR) algorithms to investigate how models of increased complexity influence prediction accuracy. The climate-sensitive models produced measurable reductions in the overall prediction bias compared to the climate-independent model across wet, dry, and average testing scenarios (3.4% vs. -27.3%) and over a 5-year holdout dataset (0.83% vs. -19.0%), with the OLS algorithm demonstrating the highest accuracy during dry conditions and enhancing the understanding of climate-demand

interactions. The model accuracy vs. complexity comparison identified the OLS algorithm as the ideal balance between interpretability and prediction accuracy.

Applying data-driven ML techniques in the climate-sensitive modeling workflow demonstrated significant improvements in model accuracy compared to traditional econometric-based climate-independent models and highlights opportunities for future work to advance water system management. We encourage future research to apply the climate-sensitive ML framework to other municipal water systems, where there may be stronger non-linear predictor-demand relationships that favor more complex ML algorithms. Additional research opportunities include applying probabilistic algorithms, exploring ensemble modeling strategies, and further decomposing service area water use to advance climate-sensitive demand modeling workflows.

Given the projected changes in supply from a changing climate, the demonstrated improvements in monthly, seasonal, and annual water demand prediction accuracy using more complex climate-sensitive water demand estimation frameworks demonstrate the capabilities to advance water system management and enhance resilience to climate vulnerabilities.

## DATA AVAILABILITY

This research uses open-source Python v3.8.5 software for all ML applications and the models are at the following GitHub: <https://github.com/whitelightning450/Water-Demand-Forecasting>. The repository contains all data to train and run the CSD-WDM.

## SUPPORTING INFORMATION

“Additional supporting information may be found online under the Supporting Information tab for this article: a description of the land-cover feature engineering process and figures describing Salt Lake City Department of Public Utilities water use.”

## ACKNOWLEDGEMENTS

This study is made possible by collaborative dedication to integrating climate resilience into water resource management by the Salt Lake City Department of Public Utilities, the University of Utah Climate Vulnerability Group, and the Alabama Water Institute. Funding for this project was provided by the National Oceanic and Atmospheric Administration (NOAA) and awarded to the Cooperative Institute for Research to Operations in Hydrology (CIROH) through the NOAA Cooperative Agreement with The University of Alabama, NA22NWS4320003.

## LITERATURE CITED

Abadi, M., Agarwal, A., Barham, P., Brevdo, E., Chen, Z., Citro, C., . . . Zheng, X. (2015). TensorFlow: Large-scale machine learning on heterogeneous systems. <https://www.tensorflow.org/>, doi: <https://doi.org/10.48550/arXiv.1603.04467>

Adamowski, J., & Karapatki, C. (2010). Comparison of multivariate regression and artificial neural networks for peak urban water-demand forecasting: Evaluation of different ann learning algorithms. *Journal of Hydrologic Engineering*, 15, 729-743. doi:10.1061/ΔASCEHE.1943-5584.0000245

Al-Jarrah, O. Y., Yoo, P. D., Muhaidat, S., Karagiannidis, G. K., & Taha, K. (2015). Efficient machine learning for big data: A review. *Big Data Research*, 2 (3), 87–93, doi: <https://doi.org/10.1016/j.bdr.2015.04.001>

Al-Sulttani, A. O., Al-Mukhtar, M., Roomi, A. B., Farooque, A. A., Khedher, K. M., & Yaseen, Z. M. (2021). Proposition of new ensemble data-intelligence models for surface water quality prediction. *IEEE Access*, 9, doi: 0.1109/ACCESS.2021.3100490

Altunkaynak, A., & Assefa, T. (2018). Monthly water demand prediction using wavelet transform, first-order differencing and linear detrending techniques based on multilayer perceptron models. *Urban Water Journal*, 15, 1-5. doi: 10.1080/1573062X.2018.1424219

Antunes, A., Andrade-Campos, A., Sardinha-Lourenco, A., & Oliveira, M. (2018). Short-term water demand forecasting using machine learning techniques. *Journal of Hydroinformatics*, 20, doi: 10.2166/hydro.2018.163

Arandia, E., Ba, A., Eck, B., & McKenna, S. (2015). Tailoring seasonal time series models to forecast short-term water demand. *Journal of Water Resources Planning and Management*, 142, 04015067. doi: 10.1061/(ASCE)WR.1943-5452.0000591

Barceló, P., Monet, M., Pérez, J., & Subercaseaux, B. (2020). Model interpretability through the lens of computational complexity. *Advances in neural information processing systems*, 33, 15487–15498, ISBN: 9781713829546

Behboudian, S., Tabesh, M., Falahnezhad, M., & Alavian Ghavanini, F. (2014, 02). A long-term prediction of domestic water demand using preprocessing in artificial neural network. *Aqua*, 63, 31. doi: 10.2166/aqua.2013.085

Biau, G., & Scornet, E. (2016). A random forest guided tour. *Test*, 25 (2), 197–227, doi: <https://doi.org/10.1007/s11749-016-0481-7>

Billings, B., & Jones, C. (2011). *Forecasting urban water demand* (3rd ed.). Denver, CO: American Waterworks Association, ISBN: 9781613000700

Blanc, E., Strzepek, K., Schlosser, A., Jacoby, H., Gueneau, A., Fant, C., . . . Reilly, J. (2014). Modeling u.s. water resources under climate change. *Earth's Future*, 2 (4), 197-224. doi: 24–<https://doi.org/10.1002/2013EF000214>

Bohne, L., Strong, C., & Steenburgh, W. J. (2020). Climatology of orographic precipitation gradients in the contiguous western united states. *Journal of Hydrometeorology*, 21 (8), 1723– 1740, doi: <https://doi.org/10.1175/JHM-D-19-0229.1>

Brooks, P. D., Gelderloos, A., Wolf, M. A., Jamison, L. R., Strong, C., Solomon, D. K., . . . others (2021). Groundwater-mediated memory of past climate controls water yield in snowmelt-dominated catchments. *Water Resources Research*, 57 (10), doi: 10.1029/2021WR030605.

Brown, C., Ghile, Y., Laverty, M., & Li, K. (2012). Decision scaling: Linking bottom-up vulnerability analysis with climate projections in the water sector. *Water Resources Research*, 48 (9), doi: 10.1029/2011WR011212

Brown, T. C., Mahat, V., & Ramirez, J. A. (2019). Adaptation to future water shortages in the united states caused by population growth and climate change. *Earth's Future*, 7 (3), 219–234, doi: <https://doi.org/10.1029/2018EF001091>

Buitinck, L., Louppe, G., Blondel, M., Pedregosa, F., Mueller, A., Grisel, O., . . . Varoquaux, G. (2013). API design for machine learning software: experiences from the scikit-learn project. CoRR, doi: <https://doi.org/10.48550/arXiv.1309.0238>

Cai, J., Luo, J., Wang, S., & Yang, S. (2018). Feature selection in machine learning: A new perspective. *Neurocomputing*, 300, 70–79, doi: <https://doi.org/10.1016/j.neucom.2017.11.077>

Census. (2023). Accessed June 2023, Population and housing unit counts (Tech. Rep.). U.S. Department of Commerce. Retrieved from <https://www.census.gov/quickfacts/saltlakecitycityutah>

Chen, G., Long, T., Xiong, J., & Bai, Y. (2017b). Multiple random forests modelling for urban water consumption forecasting. *Water Resources Management*. doi: 10.1007/s11269-017-1774-7

Chen, X.-w., & Jeong, J. C. (2007). Enhanced recursive feature elimination. In *Sixth international conference on machine learning and applications (ICMLA 2007)* (pp. 429–435), doi: 10.1109/ICMLA.2007.35

Christensen, N. S., Wood, A. W., Voisin, N., Lettenmaier, D. P., & Palmer, R. N. (2004). The effects of climate change on the hydrology and water resources of the Colorado river basin. *Climatic change*, 62, 337–363, doi: <https://doi.org/10.1023/B:CLIM.0000013684.13621.1f>

Collins, B., & Associates. (2019). 2018 supply and demand master plan (Tech. Rep.). Salt Lake City, Utah: BCA.

Coomes, P., Kornstein, B., Rockaway, T., & Rivard, J. (2010, 01). North America residential water usage trends. *Proceedings of the Water Environment Federation*, 2010, 6488-6500. doi: 10.2175/193864710798206892

CWCB. (2015). Colorado's water plan (Tech. Rep.). Denver, Colorado: Colorado Water Conservation Board.

Dawadi, S., & Ahmad, S. (2012). Changing climatic conditions in the colorado river basin: Implications for water resources management. *Journal of Hydrology*, 430, 127–141, doi: <https://doi.org/10.1016/j.jhydrol.2012.02.010>

Desai, S., & Ouarda, T. B. (2021). Regional hydrological frequency analysis at ungauged sites with random forest regression. *Journal of Hydrology*, 594, 125861, doi: <https://doi.org/10.1016/j.jhydrol.2020.125861>

Dieter, C. A. (2018). Water availability and use science program: Estimated use of water in the united states in 2015. Geological Survey, ISBN: 9781411342330

Donkor, E., Mazzuchi, T., Soyer, R., & Roberson, A. (2014, 02). Urban water demand forecasting: Review of methods and models. *Journal of Water Resources Planning and Management*, 140, 146-159. doi: 10.1061/(ASCE)WR.1943-5452.0000314

Donnelly, K., & Cooley, H. (2015). Water use trends. Pacific Institute, Oakland, California, ISBN: 1893790649

Drobnič, F., Kos, A., & Pustišek, M. (2020). On the interpretability of machine learning models and experimental feature selection in case of multicollinear data. *Electronics*, 9 (5), 761, doi: <https://doi.org/10.3390/electronics9050761>

Finch, D. M., Pendleton, R. L., Reeves, M. C., Ott, J. E., Kilkenny, F. F., Butler, J. L., . . . others (2016). Rangeland drought: effects, restoration, and adaptation. Effects of drought on forests and rangelands in the United States: a comprehensive science synthesis, 155–194.

Fisher, R. (1920). Accuracy of observation, a mathematical examination of the methods of determining, by the mean error and by the mean square error. *Monthly Notices of the Royal Astronomical Society*, 80, 758–770.

Fleming, S. W., Garen, D. C., Goodbody, A. G., McCarthy, C. S., & Landers, L. C. (2021). Assessing the new natural resources conservation service water supply forecast model for the American west: A challenging test of explainable, automated, ensemble artificial intelligence. *Journal of Hydrology*, 602, 126782, doi: <https://doi.org/10.1016/j.jhydrol.2021.126782>

Ghalehkhondabi, I., Ardjmand, E., Young, W. A., & Weckman, G. R. (2017). Water demand forecasting: review of soft computing methods. *Environmental Monitoring and Assessment*, 189, 1-13, doi: <https://doi.org/10.1007/s10661-017-6030-3>

Ghiassi, M., Zimbra, D. K., & Saidane, H. (2008). Urban water demand forecasting with a dynamic artificial neural network model. *Journal of Water Resources Planning and Management*, 134 (2), 138-146. doi: 10.1061/(ASCE)0733-9496(2008)134:2(138)

Gleick, P. H. (2010). Roadmap for sustainable water resources in southwestern North America. *Proceedings of the National Academy of Sciences*, 107 (50), 21300–21305, doi: <https://doi.org/10.1073/pnas.1005473107>

Granata, F., & Di Nunno, F. (2021). Forecasting evapotranspiration in different climates using ensembles of recurrent neural networks. *Agricultural Water Management*, 255, 107040, doi: <https://doi.org/10.1016/j.agwat.2021.107040>

Guidotti, R., Monreale, A., Ruggieri, S., Turini, F., Giannotti, F., & Pedreschi, D. (2018). A survey of methods for explaining black box models. *ACM computing surveys (CSUR)*, 51 (5), 1–42, doi: <https://doi.org/10.1145/3236009>

Gupta, H. V., Kling, H., Yilmaz, K. K., & Martinez, G. F. (2009). Decomposition of the mean squared error and NSE performance criteria: Implications for improving hydrological modelling. *Journal of Hydrology*, 377 (1-2), 80–91, doi: <https://doi.org/10.1016/j.jhydrol.2009.08.003>

Hamada, M., Tanimu, J. J., Hassan, M., Kakudi, H. A., & Robert, P. (2021). Evaluation of recursive feature elimination and lasso regularization-based optimized feature selection approaches for cervical cancer prediction. In 2021 IEEE 14th international symposium on

embedded multicore/many-core systems-on-chip (MCSOC) (pp. 333–339), doi: 10.1109/MCSOC51149.2021.00056

Hastie, T., Tibshirani, R., Friedman, J. H., & Friedman, J. H. (2009). The elements of statistical learning: data mining, inference, and prediction (Vol. 2). Springer, ISBN: 978-0-387-21606-5

Hirsch, R. (2011). A perspective on nonstationarity and water management. *Journal of the American Water Resources Association*, 47, 436 - 446. doi: 10.1111/j.1752-1688.2011.00539.x

Hughes, D. A., & Smakhtin, V. (1996). Daily flow time series patching or extension: a spatial interpolation approach based on flow duration curves. *Hydrological Sciences Journal*, 41 (6), 851-871, doi: 10.1080/02626669609491555

Jacobs, H., & Haarhoff, J. (2007, 12). Prioritisation of parameters influencing residential water use and wastewater flow. *Journal of Water Supply Research and Technology-aqua - J WATER SUPPLY RES TECHNOL-AQ*, 56. doi: 10.2166/aqua.2007.068

Khatri, K. B., Strong, C., Kochanski, A. K., Burian, S., Miller, C., & Hasenjager, C. (2018). Water resources criticality due to future climate change and population growth: Case of river basins in Utah, USA. *Journal of Water Resources Planning and Management*, 144 (8), 04018041, doi: [https://doi.org/10.1061/\(ASCE\)WR.1943-5452.0000959](https://doi.org/10.1061/(ASCE)WR.1943-5452.0000959)

Knoben, W. J., Freer, J. E., & Woods, R. A. (2019). Inherent benchmark or not? Comparing nash-sutcliffe and kling-gupta efficiency scores. *Hydrology and Earth System Sciences*, 23 (10), 4323–4331, doi: <https://doi.org/10.5194/hess-23-4323-2019>

Koutsoyiannis, D., & Montanari, A. (2014). Negligent killing of scientific concepts: The stationarity case. *Hydrological Sciences Journal*, 60, 150527103244004. doi: 10.1080/02626667.2014.959959

Lee, M., Tansel, B., & Balbin, M. (2011). Influence of residential water use efficiency measures on household water demand: A four-year longitudinal study. *Resources, Conservation and Recycling*, 56, 1-6. doi: 10.1016/j.resconrec.2011.08.006

Li, J., Wang, Z., Wu, X., Xu, C.-Y., Guo, S., & Chen, X. (2020). Toward monitoring short-term droughts using a novel daily scale, standardized antecedent precipitation evapotranspiration index. *Journal of Hydrometeorology*, 21 (5), 891–908, doi: <https://doi.org/10.1175/JHM-D-19-0298.1>

Li, W., & Huicheng, Z. (2010). Urban water demand forecasting based on HP filter and fuzzy neural network. *Journal of Hydroinformatics*, 12 (2), 172-184. doi: 10.2166/hydro.2009.082

Lin, X., Yang, F., Zhou, L., Yin, P., Kong, H., Xing, W., . . . Xu, G. (2012). A support vector machine-recursive feature elimination feature selection method based on artificial contrast variables and mutual information. *Journal of Chromatography B*, 910, 149–155, doi: <https://doi.org/10.1016/j.jchromb.2012.05.020>

Makridakis, S., Spiliotis, E., & Assimakopoulos, V. (2018). Statistical and machine learning forecasting methods: Concerns and ways forward. *PloS one*, 13 (3), e0194889, doi: <https://doi.org/10.1371/journal.pone.0194889>

Matthews, J., Wickel, B., & St. George Freeman, S. (2011). Converging currents in climate relevant conservation: Water, infrastructure, and institutions. *PLoS biology*, 9, e1001159. doi: 10.1371/journal.pbio.1001159

Maupin, M. A. (2018). Summary of estimated water use in the united states in 2015 (Tech. Rep.). Washington, D.C., United States of America: US Geological Survey, doi: <https://doi.org/10.3133/fs20183035>

Milly, P. C. D., Betancourt, J., Falkenmark, M., Hirsch, R. M., Kundzewicz, Z. W., Lettenmaier, D. P., & Stouffer, R. J. (2008). Stationarity is dead: Whither water management? *Science*, 319, 573 – 574, doi: 10.1126/science.1151915

Moayedi, Hossein, Dieu Tien Bui, et al. (2019). Spotted hyena optimizer and ant lion optimization in predicting the shear strength of soil. *Applied Sciences* 9.22, p. 4738, doi: <https://doi.org/10.3390/app9224738>

Moglia, M., Cook, S., & Tapsuwan, S. (2018). Promoting water conservation: where to from here? *Water*, 10 (11), 1510, doi: <https://doi.org/10.3390/w10111510>

Mosavi, A., Sajedi Hosseini, F., Choubin, B., Goodarzi, M., Dineva, A. A., & Rafiei Sardooi, E. (2021). Ensemble boosting and bagging-based machine learning models for groundwater potential prediction. *Water Resources Management*, 35 (1), 23–37, doi: <https://doi.org/10.1007/s11269-020-02704-3>

Muir, M., Luce, C., Gurrieri, J., Matyjasik, M., Bruggink, J., Weems, S., . . . Leahy, S. (2018). Effects of climate change on hydrology, water resources, and soil. Washington, DC: USDA Forest Service. Gen. Tech. Rep. RMRS-GTR-375

Naz, B. S., Kao, S.-C., Ashfaq, M., Gao, H., Rastogi, D., & Gangrade, S. (2018). Effects of climate change on streamflow extremes and implications for reservoir inflow in the United States. *Journal of Hydrology*, 556, 359–370, <https://doi.org/10.1016/j.jhydrol.2017.11.027>

NOAA. (2023). Accessed May 2023, Mesowest alta guard current conditions. <https://www.wrh.noaa.gov/mesowest/getobext.php>.

Olmstead, S. M. (2014). Climate change adaptation and water resource management: A review of the literature. *Energy Economics*, 46, 500–509, doi: <https://doi.org/10.1016/j.eneco.2013.09.005>

Opalinski, N. F., Bhaskar, A. S., & Manning, D. T. (2020). Spatial and seasonal response of municipal water use to weather across the contiguous us. *Journal of the American Water Resources Association*, 56 (1), 68–81, doi: <https://doi.org/10.1111/1752-1688.12801>

Oyebode, O., & Ighravwe, D. E. (2019). Urban water demand forecasting: A comparative evaluation of conventional and soft computing techniques. *Resources*, 8 (3), 156. Retrieved from <http://dx.doi.org/10.3390/resources8030156> doi: 10.3390/resources8030156

Parker, J. M., & Wilby, R. L. (2013). Quantifying household water demand: a review of theory and practice in the UK. *Water Resources Management*, 27 (4), 981–1011, doi: <https://doi.org/10.1007/s11269-012-0190-2>

Pedregosa, F., Varoquaux, G., Gramfort, A., Michel, V., Thirion, B., Grisel, O., . . . others (2011). Scikit-learn: Machine learning in python. *Journal of machine learning research*, 12 (10), 2825-2830, CRID: 1370005891170856713

Peters-Lidard, C. D., Rose, K. C., Kiang, J. E., Strobel, M. L., Anderson, M. L., Byrd, A. R., . . . Arndt, D. S. (2021). Indicators of climate change impacts on the water cycle and water management. *Climatic Change*, 165, 1–23, doi: <https://doi.org/10.1007/s10584-021-03057-5>

Pham, Binh Thai, Chongchong Qi, et al. (2020). A novel hybrid soft computing model using random forest and particle swarm optimization for estimation of undrained shear strength of soil. *Sustainability* 12.6, p. 2218, doi: <https://doi.org/10.3390/su12062218>

Polebitski, A., Palmer, R., & Waddell, P. (2011). Evaluating water demands under climate change and transitions in the urban environment. *Journal of Water Resources Planning and Management*, 137 (3), 249-257. doi: 10.2495/EC070011

Polebitski, A. S., & Palmer, R. N. (2010). Seasonal residential water demand forecasting for census tracts. *Journal of Water Resources Planning and Management*, 136 (1), 27-36. doi: 10.1061/(ASCE)WR.1943-5452.0000003

Potts, D., Huxman, T., Cable, J., English, N., Ignace, D., Eilts, J., . . . Williams, D. (2006). Antecedent moisture and seasonal precipitation influence the response of canopy-scale carbon and water exchange to rainfall pulses in a semi-arid grassland. *New Phytologist*, 170 (4), 849–860, doi: <https://doi.org/10.1111/j.1469-8137.2006.01732.x>

Quilty, J., Adamowski, J., & Boucher, M.-A. (2019). A stochastic data-driven ensemble forecasting framework for water resources: A case study using ensemble members derived from a database of deterministic wavelet-based models. *Water Resources Research*, 55 (1), 175– 202, doi: <https://doi.org/10.1029/2018WR023205>

Rajagopalan, B., Nowak, K., Prairie, J., Hoerling, M., Harding, B., Barsugli, J., . . . Udall, B. (2009). Water supply risk on the colorado river: Can management mitigate? *Water Resources Research*, 45 (8), doi: <https://doi.org/10.1029/2008WR007652>

Riter, A., & Munoz-Carpena, R. (2013). Performance evaluation of hydrological models: Statistical significance for reducing subjectivity in goodness-of-fit assessments. *Journal of Hydrology*, 480, 33 - 45. doi: <https://doi.org/10.1016/j.jhydrol.2012.12.004>

Rodriguez -Galiano, V., Ghimire, B., Rogan, J., Chica-Olmo, M., & Rigol-Sanchez, J. (2012). An assessment of the effectiveness of a random forest classifier for land-cover classification.

ISPRS Journal of Photogrammetry and Remote Sensing, 67, 93–104. doi: 10.1016/j.isprsjprs.2011.11.002

Rosenberg, E. A., Wood, A. W., & Steinemann, A. C. (2011). Statistical applications of physically based hydrologic models to seasonal streamflow forecasts. *Water Resources Research*, 47 (3), doi:10.1029/2010WR010101

Ryu, J. H., Contor, B., Johnson, G., Allen, R., & Tracy, J. (2012). System dynamics to sustainable water resources management in the eastern snake plain aquifer under water supply uncertainty. *JAWRA Journal of the American Water Resources Association*, 48 (6), 1204–1220, doi: <https://doi.org/10.1111/j.1752-1688.2012.00681.x>

Salt Lake City Department of Public Utilities. (2022). Accessed July 2022. Water rates - slcdocs.com. Salt Lake City Department of Public Utilities. <http://www.slcdocs.com/utilities/PDF%20Files/UtilityRates/WaterrateswebCurrent.pdf>

Salt Lake County. (2021). Accessed March 2021. Water conservation in salt lake county. Salt Lake County. Retrieved from <https://slco.org/water-conservation/#:~:text=Salt%20Lake%20County%20operations%2cutuntil%20May%202015%20or%20later>.

Scalzitti, J., Strong, C., & Kochanski, A. K. (2016). A 26-year high-resolution dynamical downscaling over the Wasatch mountains: Synoptic effects on winter precipitation performance. *Journal of Geophysical Research: Atmospheres*, 121 (7), 3224-3240. doi: 10.1002/2015JD024497

Schewe, J., Heinke, J., Gerten, D., Haddeland, I., Arnell, N., Clark, D., . . . Kabat, P. (2014). Multimodel assessment of water scarcity under climate change. *Proceedings of the National Academy of Sciences of the United States of America*, 111, 3245-3250. doi: 10.1073/pnas.1222460110

Seabold, S., & Perktold, J. (2010, 01). Statsmodels: Econometric and statistical modeling with python. *PROC. OF THE 9th PYTHON IN SCIENCE CONF.* (2010), 92-96. doi: 10.25080/Majora-92bf1922-011

Shrestha, A., & Mahmood, A. (2019). Review of deep learning algorithms and architectures. *IEEE Access*, 7, 53040–53065, doi: 10.1109/ACCESS.2019.2912200

Shukla, S., Steinemann, A. C., & Lettenmaier, D. P. (2011). Drought monitoring for Washington state: Indicators and applications. *Journal of Hydrometeorology*, 12 (1), 66–83, doi: <https://doi.org/10.1175/2010JHM1307.1>

Sit, M., Demiray, B. Z., Xiang, Z., Ewing, G. J., Sermet, Y., & Demir, I. (2020). A comprehensive review of deep learning applications in hydrology and water resources. *Water Science and Technology*, 82 (12), 2635–2670, doi: <https://doi.org/10.2166/wst.2020.369>

Smith, K., Strong, C., & Wang, S.-Y. (2015). Connectivity between historical great basin precipitation and pacific ocean variability: A cmip5 model evaluation. *Journal of Climate*, 28, 150520110052002. doi: 10.1175/JCLI-D-14-00488.1

SNWA. (2019). Joint water conservation plan (Tech. Rep.). Las Vegas, Nevada: Southern Nevada Water Authority.

Snyder, K. A., Evers, L., Chambers, J. C., Dunham, J., Bradford, J. B., & Loik, M. E. (2019). Effects of changing climate on the hydrological cycle in cold desert ecosystems of the great basin and Columbia plateau. *Rangeland Ecology & Management*, 72 (1), 1–12, doi: <https://doi.org/10.1016/j.rama.2018.07.007>

Song, P., & Kroll, C. (2011). The impact of multicollinearity on small sample hydrologic regional regression. *Water Resources Research*, 49, 3713-3722. doi: 10.1061/41173(414)389

Stern, C. V., & Sheikh, P. A. (2021). Management of the Colorado river: Water allocations, drought, and the federal role. Congressional Research Service. CRS: R45546, URL: [https://www.everycrsreport.com/files/20190321\\_R45546\\_bbcb0e946b7f42c8c312e2070e766cbeccff0c0ee.pdf](https://www.everycrsreport.com/files/20190321_R45546_bbcb0e946b7f42c8c312e2070e766cbeccff0c0ee.pdf)

Strobl, C., Boulesteix, A.-L., Kneib, T., Augustin, T., & Zeileis, A. (2008). Conditional variable importance for random forests. *BMC Bioinformatics*, 9, 1–11, doi: <https://doi.org/10.1186/1471-2105-9-307>

Tiwari, M. K., & Adamowski, J. (2014). Medium-term urban water demand forecasting with limited data using an ensemble wavelet–bootstrap machine-learning approach. *Journal of Water Resources Planning and Management*, 141. doi: 10.1061/(ASCE)WR.1943-5452.0000454

Tolosi, L., & Lengauer, T. (2011). Classification with correlated features: unreliability of feature ranking and solutions. *Bioinformatics*, 27 (14), 1986–1994, doi: <https://doi.org/10.1093/bioinformatics/btr300>

Towler, E., Roberts, M., Rajagopalan, B., & Sojda, R. (2013). Incorporating probabilistic seasonal climate forecasts into river management using a risk-based framework. *Water Resources Research*, 49. doi: 10.1002/wrcr.20378

Tyralis, H., Papacharalampous, G., & Langousis, A. (2019). A brief review of random forests for water scientists and practitioners and their recent history in water resources. *Water*, 11 (5). doi: 10.3390/w11050910

UDNR. (2010). Jordan river basin planning for the future (Tech. Rep.). Utah Division of Water Resources. Retrieved from <https://water.utah.gov/wp-content/uploads/2019/SWP/JordanRiver/Jordan-River-Basin-Final2010.pdf>

UDWR. (2019). 2015 municipal and industrial water use data (Tech. Rep.). Utah Division of Water Resources. Retrieved from <https://water.utah.gov/wp-content/uploads/2019/BasinPlanning/PDF/2015WaterData.pdf>

UDWR. (2019). Utah's regional M & I water conservation goals (Tech. Rep.). UDNR. Retrieved from <https://water.utah.gov/wp-content/uploads/2019/12/Regional-Water-Conservation-Goals-Report-Final.pdf>

UDWR. (2023). Water records/use information (Tech. Rep.). Salt Lake City, Utah: Utah Division of Water Rights. Retrieved from <https://waterrights.utah.gov/wateruse/WaterUseList.asp>

USBR (2023). Accessed June 2023, National inventory of dams. United States Bureau of Reclamation, Retrieved from <https://nid.sec.usace.army.mil/#/>

U.S. EPA. (1998). Water conservation plan guidelines (Tech. Rep.). Washington, D.C.: U.S. Environmental Protection Agency.

USGS. (2019a). Landsat 5. United States Geological Service, Retrieved from [https://developers.google.com/earth-engine/datasets/catalog/LANDSAT\\_LT05\\_C01\\_T1\\_SR](https://developers.google.com/earth-engine/datasets/catalog/LANDSAT_LT05_C01_T1_SR)

USGS. (2019b). Landsat 8. United States Geological Service, Retrieved from [https://developers.google.com/earth-engine/datasets/catalog/LANDSAT\\_LC08\\_C01\\_T1\\_SR](https://developers.google.com/earth-engine/datasets/catalog/LANDSAT_LC08_C01_T1_SR)

UDNR. (2014). State of Utah municipal and industrial water supply and use study summary 2010 (Tech. Rep.). Utah Department of Natural Resources, Retrieved from <https://water.utah.gov/wp-content/uploads/2019/03/2010-MI-Statewide-SummaryCH.pdf>

Vijai, P., & Sivakumar, B. (2018). Performance comparison of techniques for water demand forecasting. *Procedia Computer Science*, 143, 258 - 266. (8th International Conference on Advances in Computing & Communications (ICACC-2018)) doi: <https://doi.org/10.1016/j.procs.2018.10.394>

Wang, Y., Ocampo-Martinez, C., & Puig, V. (2014). Gaussian-process-based demand forecasting for predictive control of drinking water networks. 9th International Conference on Critical Information Infrastructures, doi: [https://doi.org/10.1007/978-3-319-31664-2\\_8](https://doi.org/10.1007/978-3-319-31664-2_8)

Xia, Y., Mitchell, K., Ek, M., Cosgrove, B., Sheffield, J., Luo, L., . . . Lohmann, D. (2012). Continental-scale water and energy flux analysis and validation for North American Land Data Assimilation System project phase 2 (NLDAS-2): 2. validation of model-simulated streamflow. *Journal of Geophysical Research: Atmospheres*, 117 (D3). doi: 10.1029/2011JD016051

Yan, K., & Zhang, D. (2015). Feature selection and analysis on correlated gas sensor data with recursive feature elimination. *Sensors and Actuators B: Chemical*, 212, 353–363, doi: <https://doi.org/10.1016/j.snb.2015.02.025>

Zhao, G., Gao, H., Kao, S., Voisin, N., & Naz, B. (2018). A modeling framework for evaluating drought resilience of a surface water supply system under non-stationarity. *Journal of Hydrology*, 563, 22-32. doi: doi.org/10.1016/j.jhydrol.2018.05.037

Zhu, Z., Woodcock, C. E., Rogan, J., & Kellndorfer, J. (2012). Assessment of spectral, polarimetric, temporal, and spatial dimensions for urban and peri-urban land cover classification using Landsat and Sar data. *Remote Sensing of Environment*, 117, 72 - 82. *Remote Sensing of Urban Environments* doi: <https://doi.org/10.1016/j.rse.2011.07.020>

## Tables

**Table 1.** The long-term record of Salt Lake City Department of Public Utilities (SLCDPU) water use from 1980 - 2017 exhibits high seasonal (i.e., change in water use from month to month) and high interannual (i.e., large deviations of monthly use between years) variability.

Month	Minimum	Mean	Maximum	$\sigma$
Apr*	430	720	1010	140
May*	610	1110	1520	250
Jun*	1090	1720	2180	280
Jul*	1470	2070	2640	280
Aug*	1280	1930	2390	280
Sep*	1030	1440	1840	210
Oct*	600	870	1230	160
Season*	1060	1410	1690	170
Season**	79.1	105.1	125.7	13.0

\* units in lpcd

\*\* units in Mm<sup>3</sup>

**Table 2.** Historical monthly per-capita demands (lpcd) calculated using the historical water records of SLCDPU and equation 1.

Nov-Mar	Apr	Mar	Jun	Jul	Aug	Sep	Oct
590	730	1130	1750	2110	1970	1090	890

**Table 3.** The testing scenarios cover a range of climate conditions from wet to dry and display how recent years have trended drier than the historical record based on annual snowfall from the Alta Guard station located in the headwaters of Little Cottonwood Canyon, Utah.

Year	Scenario Classification	Annual Snowfall (cm)	Δ Mean Snowfall (cm)	Return Interval (yrs)
2008	Wet	1,660	399	15
2015	Dry	680	-582	150
2017	Average	1,347	85	2
2018	Dry	731	-530	70
2019	Average	1,206	-56	2
2020	Average	1,056	-205	4
2021	Average	949	-312	5
2022	Dry	717	-545	85

**Table 4.** The climate-independent model demonstrates a large negative *PBias* for all testing scenarios, with dry conditions leading to greater error and reduced prediction accuracy. The climate-sensitive Ordinary Least Squared (OLS), Multilayered Perceptron (MLP), and Random Forest (RFR) models display an improvement in prediction accuracy compared to the climate-independent method. The OLS and RFR models demonstrate the most refined predictive capability of the models evaluated.

Scenario	Model	<i>Pbias</i> (%)	<i>RMSE</i> (lpcd)	<i>RMSE</i> ( $\times 10^4$ m <sup>3</sup> )	<i>KGE</i>
Total	Climate-Independent	-27.3	294	10.3	0.67
	OLS	3.4	74	2.6	0.96
	MLP	-2.5	153	5.6	0.86
	RFR	-1.7	109	4.0	0.93
Wet	Climate-Independent	-12.1	145	5.1	0.81
	OLS	6.04	93	3.2	0.89
	MLP	8.0	91	3.3	0.91
	RFR	-2.3	136	5.0	0.94
Dry	Climate-Independent	-39.7	363	12.7	0.48
	OLS	0.2	48	1.7	0.98
	MLP	-13.8	181	6.6	0.68
	RFR	-7.5	108	3.9	0.82
Average	Climate-Independent	-33.4	330	11.5	0.62
	OLS	3.3	74	2.6	0.96
	MLP	-4.3	170	6.2	0.84
	RFR	3.6	73	2.7	0.94
2018-2022	Climate-Independent	-19.0	293	10.7	0.66
	OLS	0.8	165	6.0	0.79
	MLP	-6.0	237	8.7	0.62
	RFR	0.003	172	6.3	0.81

**Table 5.** All climate-sensitive models demonstrate a large percentage reduction in error compared to the climate-independent model. Seasonal water use refers to the period between April and October of increased outdoor water demand.

Scenario	Model	Annual Prediction (Mm <sup>3</sup> )	Annual Error (%)	Seasonal Prediction (Mm <sup>3</sup> )	Seasonal Error (%)
Wet	Climate-Independent	135	6.2	108.0	7.9
	OLS	112	-16.9	92.4	-99.0
	MLP	117	-10.6	91.9	-6.5
	RFR	123	-5.8	97.5	1.7
Dry	Climate-Independent	135	36.1	108.0	34.0
	OLS	101	-0.8	78.8	0.1
	MLP	116	10.1	93.7	17.6
	RFR	110	5.6	87.4	9.9
Average	Climate-Independent	135	30.8	108.0	31.4
	OLS	104	-2.8	82.4	1.0
	MLP	112	0.8	90.0	8.5
	RFR	109	0.5	87.9	8.0
2018-2022	Climate-Independent	135	20.2	108.0	21.7
	OLS	112	-4.8	90.3	3.6
	MLP	120	-0.2	97.9	11.6
	RFR	113	-3.7	91.1	5.5

\* 5-year average

**Table 6.** The Correlation Bias Reduction with Recursive Feature Elimination (CBR-RFE) feature selection process identifies the optimal predictors of monthly per-capita demand. Using the predictors in the Ordinary Least Squares (OLS) algorithm communicates the statistical relationships to the respective monthly demands with the respective variable coefficients as shown below.

Predictor	Apr	May	Jun	Jul	Aug	Sep	Oct
Population Density <sup>1</sup>				-0.3	-0.1		
Mar LCC Streamflow <sup>2</sup>	-0.2				0.2		
Apr LCC Streamflow <sup>2</sup>	0.1				0.1		
May LCC Streamflow <sup>2</sup>					-0.4		
May BCC Streamflow <sup>2</sup>					0.2		
Season Snowfall <sup>3</sup>			11.2				
Apr Mean Temperature <sup>4</sup>	21.3		33.3	-16.0	22.5	11.7	15.8
Apr Precipitation <sup>5</sup>	-1.2				-1.1		
May Mean Temperature <sup>4</sup>		54.1	56.0	36.1	45.4	12.4	-7.9
May Precipitation <sup>5</sup>		-4.0					
Jun Mean Temperature <sup>4</sup>					3.1	-14.9	
Jun Precipitation <sup>5</sup>			-7.4		1.5		
Jul Mean Temperature <sup>4</sup>				118.5	3.5	-28.2	
Aug Mean Temperature <sup>4</sup>					58.5	45.9	
Aug Precipitation <sup>5</sup>					-6.8		
Sep Mean Temperature <sup>4</sup>						30.7	
Sep Precipitation <sup>5</sup>						-3.6	
Oct Mean Temperature <sup>4</sup>							21.6

<sup>1</sup> change in lpcd per persons/km<sup>2</sup>

<sup>2</sup> change in lpcd per cms of streamflow ( $\times 10^{-4}$ )

<sup>3</sup> change in lpcd per cm of snow

<sup>4</sup> change in lpcd per °C

<sup>5</sup> change in lpcd per mm of liquid precipitation

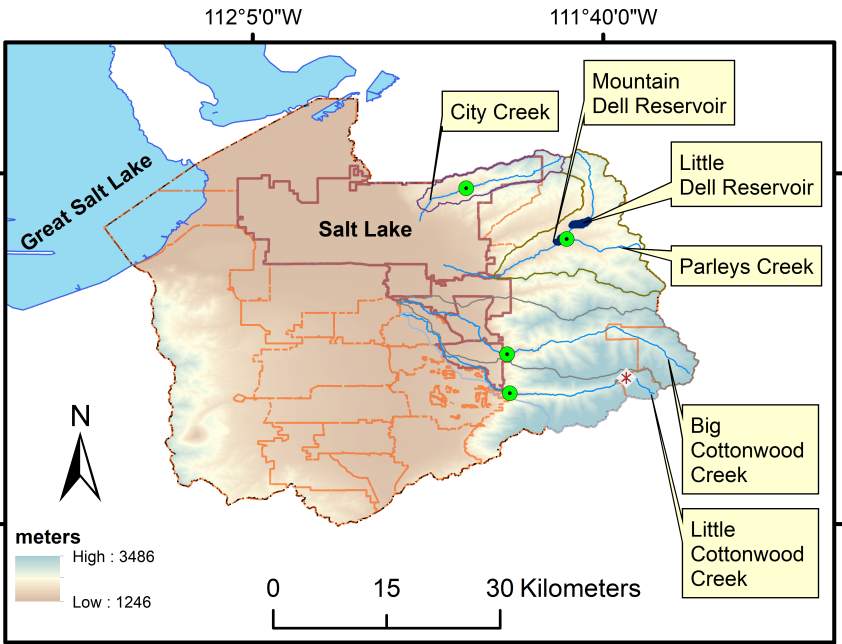
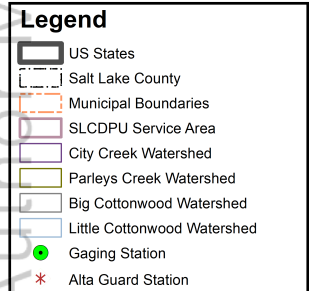
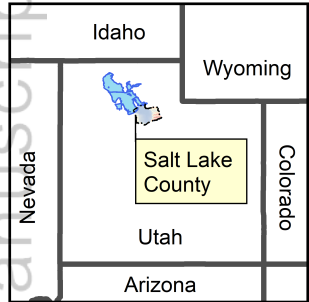
## Figure Captions

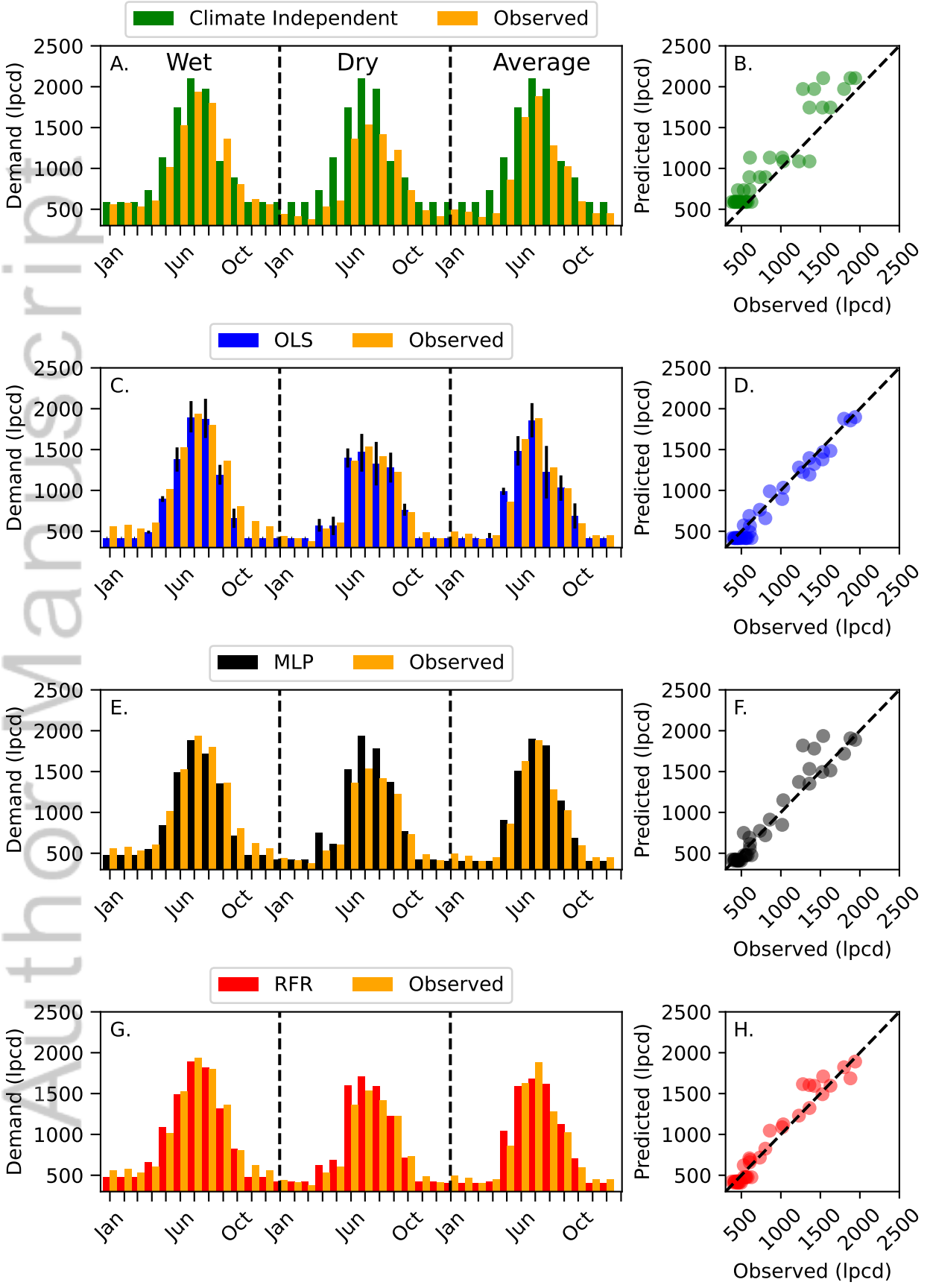
**Figure 1.** The Salt Lake City Department of Public Utilities (SLCDPU) provides constituents with high-quality snowpack-driven surface water supplies (i.e., up to 60% of the annual supply) from four key watersheds in the adjacent Wasatch Mountains (Collins & Associates, 2019).

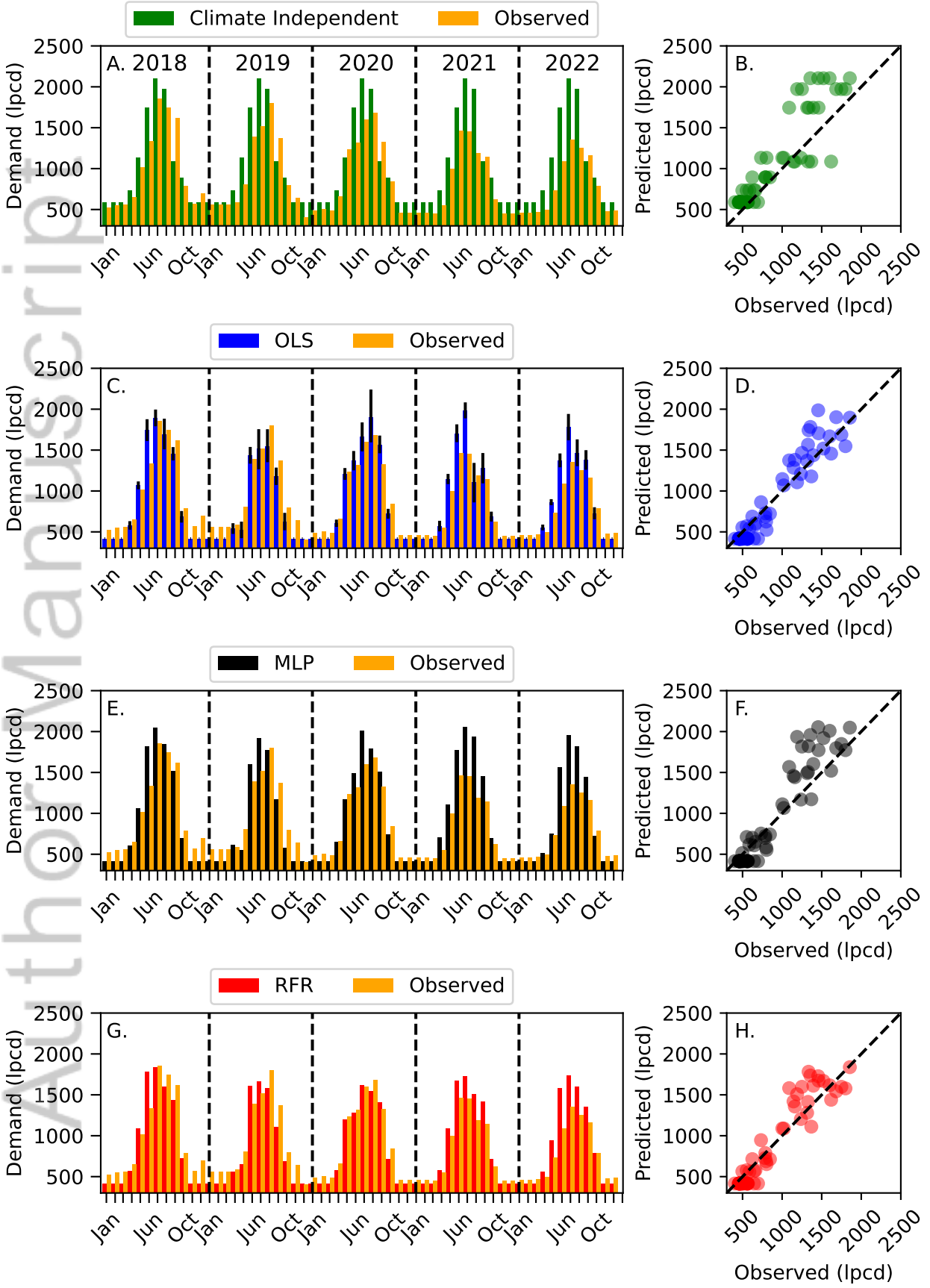
**Figure 2.** The climate-independent model exhibits an average  $-27\% PBias$  (A., B.) across all climate scenarios, with drought conditions severely challenging the prediction accuracy of the model. The climate-sensitive models (C. - H.) display a prediction accuracy improvement for wet, dry, and average climate conditions. The Ordinary Least Squares (OLS) (C., D.) and Random Forest (RFR) (G., H.) capture the influences of climate on municipal water demands with improved prediction skill compared to the multilayered perceptron model (MLP) (E., F.). The black error bars within the OLS predictions (C.) communicate the April to October predictions to a 95% confidence interval.

**Figure 3.** The climate-independent model exhibits an average  $-19\% PBias$  (A., B.) across the 2018-2022 forecast period, with the average and dry conditions of 2021 and 2022, respectively, challenging model accuracy to a greater degree than the other years. The climate-sensitive models (C. - H.) display a prediction accuracy improvement for the dry and average climate conditions experienced during the 2018-2022 period, with the OLS (C., D.) and RFR (G., H.) demonstrating greater prediction skill than the MLP model, which tends to over predict demands ( $PBias -6.0\%$ ). The black error bars within the OLS predictions (C.) communicate the April to October predictions to a 95% confidence interval.

**Figure 4.** By varying the monthly air temperature and precipitation as percentages of normal within the bounds of the historical record, the climate-sensitive OLS model can produce a range of annual volumetric demands reflecting the influences of dynamic climate conditions to support proactive water system management.







# Author Manuscript

